
Invariant backpropagation: how to train a transformation-invariant neural network

Sergey Demyanov
James Bailey
Ramamohanarao Kotagiri
Christopher Leckie

S.DEMYANOV@STUDENT.UNIMELB.EDU.AU
BAILEYJ@UNIMELB.EDU.AU
KOTAGIRI@UNIMELB.EDU.AU
CALECKIE@UNIMELB.EDU.AU

Department of Computing and Information Systems, The University of Melbourne, Parkville, VIC, Australia, 3010

Abstract

In supervised learning, the nature of data often implies that the vast majority of transformations of the feature vectors, such as translation, scaling and rotation for images, do not change an object's class. At the same time, neural networks are known to be sensitive to such variations of input vectors. We propose an extension of the backpropagation algorithm that incorporates this information in the learning process, so that the neural network predictions are robust to variations and noise in the feature vector. This extension consists of an additional forward pass performed on the derivatives that are obtained in the end of the backward pass. We apply our algorithm to a collection of datasets for image classification, confirm its theoretically established properties and demonstrate an improvement of the classification accuracy with respect to the standard backpropagation algorithm in the majority of cases.

1. Introduction

Neural networks are widely used in machine learning. For example, they are showing the best results in image classification (Szegedy et al., 2014; Lee et al., 2014), image labelling (Karpathy & Fei-Fei, 2014) and speech recognition (Deng et al., 2013). Deep neural networks applied to large datasets can automatically learn a huge number of features, that allow them to represent very complex relations between raw input data and output classes. However, it also means that deep neural networks can suffer from overfitting, and different regularization techniques are crucially important for good performance.

It is often the case that there exist a number of variations of a given object that preserve its label. For example, image labels are usually invariant to small variations in their location on the image, size and rotation. In the area of voice recognition the result has to be invariant to the speech tone, speed and accent. Moreover, the predictions should be always robust to random noise. However, this knowledge is not incorporated in the learning process.

In this work we propose a method of achieving transformation invariance, that **analytically** enforces robustness of predictions to **all types** of variations in the input vector, which are not related with its class. As an extension of the original backpropagation algorithm, it can be applied to all types of neural networks in combination with any other regularization technique. We call this algorithm **invariant backpropagation**, or simply **IBP**.

2. Related work

A number of different regularization techniques for neural networks have been proposed in recent times. One of them is dropout (Hinton et al., 2012), that acts as an ensemble of many neural networks with similar structure, each trained on a separate training set. It is easy to implement and does not increase training time. Its further development is drop-connect (Wan et al., 2013), that was claimed to have better performance, but requires much more memory. Other methods include weight decay, reducing learning rate and early stopping. As implicit regularization methods, a special types of layers are employed. For example, convolutional layers (LeCun et al., 1998) are widely used for image classification, where the input features have a spatial locality measure. They may be considered as fully connected layers, where most of the weights are zero and others are shared. It enables a significant reduction in the number of weights, preventing the network from overfitting. Good results have been shown for the combination of convolutional layers with small size multilayer perceptrons (Lin et al., 2014), which give more flexibility than pure convolutional layers. Pooling layers do not have tuned weights at all: they

Code for IBP and all experiments is available at <http://github.com/sdemyanov/ConvNet>

use this locality measure to reduce the number of features on the next layer. A recently proposed method of stochastic pooling (Zeiler & Fergus, 2013) is another example of regularization, which is similar in its nature to dropout.

Some methods directly target the problem of transformation invariance. In the case of image classification it is partially solved by convolutional neural networks (CNN), which contain convolutional layers followed by scaling layers. This combination yields translation invariance, but remains sensitive to other types of variations. Another way to solve it is to use known invariant transformations to generate additional samples and add them to the training set. However, the number of such transformations usually is very high and not all of them have a convenient analytical form that could be used for generation. Moreover, each new training object requires additional processing time.

The problem can also be split on two parts: in the first part we obtain an invariant representation and in the second part we use it for classification. There exist a number of methods that can be used for the first part. The idea of weight sharing as in CNNs was also used in Restricted Boltzmann Machines (Norouzi et al., 2009) to learn shift-invariant features. Another popular approach is to use contractive autoencoders (Rifai et al., 2011), which penalize a learned representation for high sensitivity to input variations. Other unsupervised neural net architectures have also shown an ability to learn invariant object representations (Ranzato et al., 2007). Some models are able to deal with only a particular type of transformation, like scale-invariant learning (Fergus et al., 2003) or rotation-invariant image description from LBP histograms (Ahonen et al., 2009). Two other popular tools are SIFT (Lowe, 2004) and SURF (Bay et al., 2006) features, which are invariant to translation, scale and rotation.

One more attempt to achieve transformation invariance is presented in (Simard et al., 2012). We provide a detailed overview of this article with the qualitative and quantitative comparison later in the paper.

3. Invariant backpropagation

In the first part of this section we describe the standard backpropagation algorithm, and use the introduced notation to present invariant backpropagation in the second part. Some important theoretical considerations and their practical implications for the particular layer types are represented in the third and the forth parts accordingly. The Algorithm 3.4 shows the IBP pseudo-code.

3.1. Backpropagation algorithm

We denote N as the number of layers in a neural network and y_i , $i \in \{1, \dots, N\}$ as the activation vectors of each

layer. The activation of the first layer y_1 is the feature vector. If the input is an image that consists of one or more feature maps with pixel values, we can still consider it as a vector by traversing the maps and concatenating them together. The transformation between layers might be different: convolution, matrix multiplication, non-linear transformation, etc. We assume that $y_i = f_i(y_{i-1}, w_i)$, where w_i is the set of weights, which may be empty. The computation of the layer activations is the first (forward) pass of the backpropagation algorithm.

When we solve the classification problem, we have a single label for each class. If the total number of classes is M , it is convenient to consider a 0 – 1 matrix of labels with M columns, where 1 corresponds to the correct class. In this case we can create a network that contains M neurons in the last layer, and specify the loss function as the squared loss $L = 1/2 \sum_{i=j}^M (y_N^j - y_L^j)^2$ or as the negative log-likelihood $L = - \sum_{i=j}^M y_L^j \log y_N^j$. Here y_N is the vector of values from the last layer (predictions), and y_L is the vector from the label matrix, that corresponds to the current input vector y_1 . Usually the log-likelihood loss function is applied when the network output y_N can be considered as the predictions, i.e., $\sum_1^M y_N^i = 1$. For example, this can be achieved by applying a “softmax” transformation function on the last layer.

The vector of derivatives of the loss function with respect to predictions is simply $dy_N = \partial L / \partial y_N = y_N - y_L$ for squared loss and $dy_N = -y_L / y_N$ for log loss respectively. The derivatives for the other layer activations are denoted as dy_i , $i \in \{1, \dots, N\}$. These derivatives are computed as

$$dy_{i-1} = \frac{\partial L}{\partial y_{i-1}} = \tilde{f}_i \left(\frac{\partial L}{\partial y_i}, \frac{\partial y_i}{\partial y_{i-1}} \right) = \tilde{f}_i \left(dy_i, \frac{\partial f_i}{\partial y_{i-1}}(y_{i-1}, w_i) \right). \quad (1)$$

We refer to \tilde{f}_i as the *inverse* functions of f_i . Later we show that if the function f_i is differentiable, then \tilde{f}_i is linear. The computation of activation derivatives is the second (backward) pass. At the same time we compute the derivatives of the loss function with respect to the weights

$$dw_i = \frac{\partial L}{\partial w_i} = g_i \left(\frac{\partial y_i}{\partial w_i}, \frac{\partial L}{\partial y_i} \right) = g_i \left(\frac{\partial f_i}{\partial w_i}(y_{i-1}, w_i), dy_i \right). \quad (2)$$

Usually these calculations are performed for a whole *batch* of training examples simultaneously, and the weight derivatives are averaged among the batch to reduce sample noise. After the dw_i are computed, the weights are updated: $w_i^{t+1} = w_i^t - \alpha^t \cdot dw_i^t$, $\forall i \in \{1, \dots, N\}$, $\alpha^t > 0$. Here α^t is the coefficient that specifies the size of the step in the opposite direction to the derivative, which usually reduces over time.

3.2. Overview of invariant backpropagation

In many classification problems we have a large number of features. Formally it means that the input vectors y_1 come from a high dimensional vector space. In this space every vector can move in a huge number of directions, but most of them should not change the vector's label. For example, in the image classification problem the predictions should be invariant to changes in brightness and contrast.

Note that at the end of the backward pass we obtain the vector of derivatives dy_1 . This vector defines the direction that changes the loss and therefore changes the predictions. Its length specifies how large this change is. Thus, a smaller vector length corresponds to a more robust classifier, and vice versa. Let us specify the additional loss function

$$\tilde{L} = \frac{1}{2} \|dy_1\|^2, \quad d\tilde{y}_1 = \frac{\partial \tilde{L}}{\partial dy_1} = dy_1 \quad (3)$$

which is computed at the end of the backward pass. In order to achieve transformation invariance, we need to make it as small as possible. However, absolute invariance is useless, because in this case the classifier would give the same prediction for all input vectors, increasing the value of L . Thus, we need to find a trade-off between the main loss function L and the additional loss function \tilde{L} .

Note that \tilde{L} is almost exactly the same as the Frobenius norm of the Jacobian matrix, which is used as a regularization term in contractive autoencoders (Rifai et al., 2011). Similar to it, minimization of \tilde{L} encourages the classifier to be invariant to changes of the input vector **in all directions**, not only those that are known to be invariant. At the same time, the minimization of L ensures that the predictions change when we move towards the samples of a different class, so the classifier is not invariant in these directions. Thus, the combination of these two loss functions aims to ensure good performance.

To optimise \tilde{L} , we need to look at the backward pass from another point of view. We may consider that the derivatives dy_N are the input for an *inverse* neural network that has dy_1 as its output. Indeed, all transformation functions f_i have inverse pairs \tilde{f}_i that are used to propagate the derivatives (1). If we consider these pairs as the original transformation functions, they have their own inverse pairs $\tilde{\tilde{f}}_i$. Later we show that in most cases $\tilde{\tilde{f}}_i = f_i$. Thus, we consider the derivatives as activations and the backward pass as a forward pass. As in standard backpropagation, after such a ‘‘forward’’ pass we compute the loss function \tilde{L} . The next step is also quite natural: we need to initialize the input vector y_1 with the derivatives $d\tilde{y}_1 = \partial \tilde{L} / \partial dy_1$ and perform another ‘‘backward’’ pass that has the same direction as the original forward pass. At the same time the derivatives with respect to the weights $d\tilde{w}_i = \partial \tilde{L} / \partial w_i = \tilde{g}_i(d\tilde{y}_{i-1}, dy_i)$

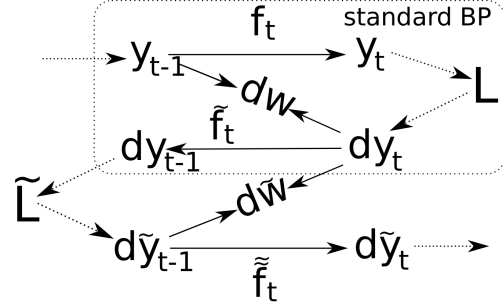


Figure 1. The scheme represents three passes if IBP algorithm. Two of them are the parts of standard backpropagation. It also shows which vectors are used for weight derivative computation.

must be computed. Fig. 1 shows the general scheme of the derivative computation. The top part corresponds to the standard backpropagation procedure.

After performing all three passes we obtain two vectors of derivatives with respect to the weights: dw and $d\tilde{w}$. Now we can define the new rule for the weight updates:

$$w^{t+1} = w^t - (\alpha^t \cdot dw^t + \beta^t \cdot d\tilde{w}^t), \quad \alpha^t \geq 0, \quad \beta^t \geq 0 \quad (4)$$

Here β is the invariance learning rate that specifies the size of the update step towards the minimization of \tilde{L} . The β/α ratio allows us to find a trade-off between two loss functions L and \tilde{L} , and plays a crucial role in achieving good performance. Note that when $\beta^t = 0$, the algorithm is equivalent to the standard backpropagation.

3.3. Theoretical details

In the previous section we explained the algorithm conceptually. Here we clarify further details.

First, notice that the forward and backward passes are performed in the same way as in the standard backpropagation algorithm. Then the additional loss function is computed, and its derivatives are used as input for the propagation on the third pass. As it is seen from (3), these derivatives $d\tilde{y}_1$ are exactly the same as the derivatives dy_1 of the main loss function L with respect to the input vector.

In the description of the algorithm in Section 3.2 we discussed the inverse functions (1) and (2) that perform the transformation $dy_{i-1} = \tilde{f}_i(dy_i, \partial f_i / \partial y_{i-1})$. By default we have to compute it for every function f_i independently, but there exists an important case of *linear* functions.

Theorem 1. *Let us assume that f_i is linear, i.e., $f_i(y_{i-1}, w_i) = y_{i-1} \cdot w_i$, where matrix multiplication is used. Then*

1. $\tilde{\tilde{f}}_i = f_i$, i.e., $d\tilde{y}_i = \tilde{\tilde{f}}_i(d\tilde{y}_{i-1}, w) = d\tilde{y}_{i-1} \cdot w_i$,
2. $\tilde{g}_i = g_i$, i.e., $d\tilde{w}_i = \tilde{g}_i(d\tilde{y}_{i-1}, dy_i) = d\tilde{y}_{i-1}^T \cdot dy_i$

Proof. In this case we know the inverse function \tilde{f}_i :

$$dy_{i-1} = \frac{\partial L}{\partial y_i} \cdot \frac{\partial y_i}{\partial y_{i-1}} = dy_i \cdot w_i^T = \tilde{f}_i(dy_i, w_i) \quad (5)$$

Note that \tilde{f} is also linear. Now let us consider the double inverse functions $\tilde{\tilde{f}}(d\tilde{y}, w)$, such that $d\tilde{y}_i = \tilde{\tilde{f}}_i(d\tilde{y}_{i-1}, w_i)$. Since the linear inverse function \tilde{f} multiplies its first argument on the transposed second argument compared with f , the same is true for the double inverse function $\tilde{\tilde{f}}$ compared with \tilde{f} , i.e.:

$$d\tilde{y}_i = \tilde{\tilde{f}}_i(d\tilde{y}_{i-1}, w_i) = d\tilde{y}_{i-1} \cdot (w_i^T)^T = d\tilde{y}_{i-1} \cdot w_i$$

It proves the part 1.

Next, in this case we know the function $g_i(y_{i-1}, dy_i)$ that computes the weight derivatives (2):

$$dw_i = \frac{\partial y_i}{\partial w_i} \cdot \frac{\partial L}{\partial y_i} = y_{i-1}^T \cdot dy_i = g_i(y_{i-1}, dy_i). \quad (6)$$

Let us again consider the backward pass \tilde{f}_i as the forward pass for the inverse net. As we stated before, the inverse function \tilde{f}_i for the linear function f_i is also linear, so the formula for derivative calculation of inverse net is also 6. However, as it follows from 5 the inverse net uses the *transposed* matrix of weights for forward propagation, so the result of derivative calculation is also transposed with respect to the matrix w_i . Also note that since dy_i acts as activations in the inverse net, we pass it as the first argument, and $d\tilde{y}_{i-1}$ as the second. Thus,

$$d\tilde{w}_i = g_i(dy_i, d\tilde{y}_{i-1})^T = (dy_i^T \cdot d\tilde{y}_{i-1})^T = d\tilde{y}_{i-1}^T \cdot dy_i,$$

and it proves the part 2. \square

Thus, we see that in the case of a linear function f_i , we propagate third pass activations the same way as we do on the first pass, i.e., multiplying them on the same matrix of weights w_i . Note that if the multiplication on weights w_i is elementwise, this may be considered as multiplication on the diagonal matrix with the values of w_i . The derivatives are also computed the same way as in the standard the BP algorithm. This allows to implement IBP using the same functions of linear layers as in the standard BP.

Furthermore, we need to establish another important property of inverse functions. Note that for any differentiable function $f(y, w)$ we can write $\tilde{f}(dy, w) = dy \cdot J(y, w)$, where $J(y, w)$ is the Jacobian matrix of the function $f(y, w)$ with respect to vector y . This immediately follows from the definition of $\tilde{f}(dy, w)$. Thus, for any differentiable function f the corresponding \tilde{f} is always linear. Moreover, if the matrix $J(y, w)$ is symmetric, then as a result of 5 we get that $\tilde{\tilde{f}}(d\tilde{y}, w) = \tilde{f}(dy, w)$.

We can also estimate the computation time for IBP. We know that convolution and matrix multiplication operations occupy almost all the processing time. As we see, our modification needs one more forward pass and one more calculation of weight derivatives. If we assume that the forward pass, backward pass and calculation of derivatives all take approximately the same time, then our modification requires about $2/3 \approx 66\%$ more time to train the network.

3.4. Implementation of the particular layer types

Here we discuss how the IBP should be implemented on the most common layer types.

A fully connected layer is a typical linear layer, which transforms its input by multiplication on the matrix of weights: $y_i = y_{i-1} \cdot w_i + u_i$, where u_i is the vector of biases. Notice that on the backward pass we do not add any bias to propagate the derivatives, so we do not add it on the third pass as well and do not compute additional bias derivatives. This is the difference between the first and the third passes. If **dropout** is used, the third pass should use the same dropout matrix as used on the first pass.

Non-linear transformation functions can be considered as a separate layer, even if they are usually implemented as a part of each layer of the other type. They do not contain weights, so we write just $f(x)$. The most common functions are: (i) sigmoid, $f(x) = 1/(1 + e^{-x})$, (ii) rectified linear unit (*relu*) (Nair & Hinton, 2010), $f(x) = \max(x, 0)$, and (iii) softmax, $f(x_i) = e^{x_i} / \sum_j e^{x_j}$. All of them are differentiable (except *relu* in 0, but it does not cause uncertainty) and have a symmetric Jacobian matrix, so the third pass is the same the backward pass. For example, in the case of the *relu* function this means that $d\tilde{y}_i = d\tilde{y}_{i-1} \cdot I(y_{i-1} > 0)$, where elementwise multiplication is used.

Convolution layers perform 2D filtering of the activation maps with the matrices of weights. Since each element of y_i is a linear combination of elements of y_{i-1} , convolution is also a linear transformation. Linearity immediately gives us $\tilde{\tilde{f}}_i(d\tilde{y}_{i-1}, w_i) = f_i(y_{i-1}, w_i)$ and $d\tilde{w}_i = d\tilde{y}_{i-1}^T \cdot dy_i$. This implies that we compute the 3rd pass layer values $d\tilde{y}_i$ in the same way as we compute the 1st pass activations y_i , by convolving with the same filter and padding. As with the fully connected layers, we do not add biases to the resulting maps and do not compute their derivatives $d\tilde{w}_i$.

The scaling layer aggregates the values over a region to a single value. Typical aggregation functions are *mean* and *max*. As it follows from the definition, both of them also perform linear transformations, so $d\tilde{y}_i = f_i(d\tilde{y}_{i-1})$. Notice that in the case of the *max* function it means that on the

third pass the same elements of $d\tilde{y}_{i-1}$ should be chosen for propagation to $d\tilde{y}_i$ as on the first pass regardless of what value they have.

Algorithm 1 Invariant backpropagation:

A single batch processing description

1. Perform standard forward and backward passes, and compute the derivatives dw for the main loss function.
 2. Perform additional forward pass using the derivatives dy_1 as activations. On this pass:
 - do not add biases to activations
 - use backward versions of non-linear functions
 - on max-pooling layers propagate the same positions as on the first pass
 3. Compute the derivatives $d\tilde{w}$ for the additional loss function \tilde{L} the same way as dw . Initialise the bias derivatives $d\tilde{w}$ to 0.
 4. Update the weights using different learning rates for dw and $d\tilde{w}$ according to the rule 4.
-

4. Alternative approaches

In fact, this is not the first attempt to use derivatives to achieve transformation invariance. In (Simard et al., 2012) the authors describe an algorithm that makes a classifier invariant to a set of *predefined* transformations. First the authors compute “*tangent*” vectors, that approximate these transformations within a local neighbourhood, i.e., $t(x, \alpha) \approx x + \alpha v(x)$ for small values of α . Here α is a transformation parameter, such as shift or rotation angle, and $v(x)$ is a tangent vector for a current sample x . After that the authors initialize the network input with a tangent vector and propagate it through the “*linearized*” network, that consists of double inverse functions \tilde{f}_i in our notation. As we have also shown, these function are always linear. For the same reasons as ours, the objective for the network output is set to be a zero vector. In this case the trained classifier does not change its predictions when the input vector is moved towards the direction of a particular tangent vector. Finally, following the standard BP, the backward pass and weight derivatives calculation is performed for this “*linearized*” network. These new derivatives are added to the main derivatives with some coefficient, the same as we do.

This tangent propagation algorithm may have appeared similar to what we propose. In both cases, the norm of the derivatives vector is minimized in order to achieve invariance to variations of the input vector. This is where the similarity ends. The basic difference lies in how the

vector of derivatives is computed. In Simard et al’s case, the classifier is trained to be invariant to only the chosen types of invariant transformations, which are given by pre-computed tangent vectors. In that case, the derivatives of the output probabilities with respect to invariant transformation parameters (such as rotation angle) are employed.

In the IBP we minimize the norm of the derivatives of the loss function L with respect to the input vector y_1 . It makes L more robust to **all** variations of y_1 , and implies the robustness of predictions y_N as well. At the same time, the minimization of L itself has the opposite effect on the classifier, so it is not invariant to moves in the directions of input space that lead to class change. There exist a huge number of elastic (non linear) transformations that do not affect image labels, but cannot be expressed as a linear combination of the basic invariant transformations, such as translation, rotation, scaling and others. In practice, the list of employed tangent vectors will always be incomplete. Thus, our method is more general than the algorithm described in (Simard et al., 2012), as it captures all variations that do not affect the label.

There also exist the differences in the implementation of both algorithms. Unlike IBP, the algorithm of Simard et al. requires tangent vectors, which need to be precomputed for each image. To do this, the authors suggest to obtain a continuous image representation by applying a Gaussian filter, requiring additional preprocessing and one more hyperparameter (filter smoothness). While the basic transformation operators are given by simple Lie operators, other transformations may require additional coding. Furthermore, each tangent vector increases training time, because the standard BP iteration must be repeated for each tangent vector. Thus, if we use 5 tangent vectors (2 for translation, 2 for scaling, 1 for rotation), we need about 6 times more time to perform training. In contrast, our algorithm always requires around 53% more time than standard BP.

We describe the results of experiments with tangent back-propagation in the next section.

5. Experiments

Since the standard backpropagation algorithm is a special case of IBP with the invariance learning rate $\beta^t = 0$ (4), we want to determine if any $\beta^0 > 0$ gives an improvement with respect to the baseline. From now on we refer to β^0 simply as β . As a baseline we considered the versions of standard BP with dropout ratio values 0 and 0.5. Dropout was always applied to the last internal fully connected layer. The best values for β were chosen by cross-validation within the training set.

We evaluated our modification on four benchmark datasets for image classification: MNIST, CIFAR-10, CIFAR-100

and SVHN. In all experiments we used the following parameters: 1) the batch size 128, 2) initial learning rate $\alpha^0 = 0.1$, 3) exponential decrease of both learning rates, i.e., $\alpha^t = \alpha^{t-1} \cdot \gamma$, $\beta^t = \beta^{t-1} \cdot \gamma$, 4) negative log-likelihood loss function, 5) *relu* nonlinear functions on internal layers, 6) *softmax* function on the last layer, 7) each convolutional layer was followed by a scaling layer with *max* aggregation function among the region of size 3×3 and stride 2.

Each dataset was first normalized to have pixel values within $[0 \ 1]$ and then the per-image mean was subtracted from each pixel (except SVHN). The SVHN dataset was normalized by applying local contrast normalization as described in (Goodfellow et al., 2013). During training each sample was randomly cropped with the following parameters: 1) cropped image size - 28px, 2) maximum shift from the central position in each dimension - 2 pixels, 3) scale range in each dimension - $[0.71 \ 1.4]$, 4) random horizontal reflection for CIFAR-10 and CIFAR-100 databases, 5) value to use if the cropped image is out of the borders of the original image - 0. Test images were centrally cropped without any random factors. After each epoch the training samples were permuted. The initial weights, cropping parameters and permutations were the same for all initial learning rates β , so the difference was only in their values. For each experiment we performed 10 attempts with different initial weights and permutations.

5.1. Datasets

Here we observe each of the benchmark datasets, describe the employed neural networks and learning parameters.

MNIST

The MNIST dataset (LeCun et al., 1998) contains handwritten digits, stored as black-and-white images of size 28×28 . The total number of classes is 10, one for each digit. There are 60000 training instances and 10000 test instances in this dataset. The network contained two convolutional layers with 32 filters of size 4×4 (padding 0) and 64 filters of size 5×5 (padding 2) and one internal FC layer of length 256. We trained the classifier for 400 epochs with the coefficient $\gamma = 0.98$, so the final learning rates were $0.98^{400} \approx 0.0003$ of the initial ones. This makes the error variance on the final epochs close to zero.

CIFAR

CIFAR-10 and CIFAR-100 (Krizhevsky, 2009) are two other popular benchmark datasets for image classification. They consist of coloured 3-channel images of size 32×32 such as cats, dogs, cars, and others. While CIFAR-10 has just 10 broad classes, CIFAR-100 has 100 more specific classes for the same images. For training we used a neural net containing 3 convolutional layers with the filter size 5×5 (padding 0, 2 and 2), and one internal FC layer of

Table 1. Mean errors for standard BP ($\beta = 0$) and invariant BP ($\beta > 0$) and the best β on different datasets, **without dropout**. * means statistically significant according to the Wilcoxon rank-sum test ($\alpha = 0.05$).

	Standard BP	Invariant BP	best β
MNIST	0.426 ± 0.068	0.384 ± 0.031 *	$2 \cdot 10^{-3}$
CIFAR-10	17.73 ± 0.376	17.31 ± 0.247 *	$5 \cdot 10^{-4}$
CIFAR-100	50.37 ± 0.321	49.60 ± 0.437 *	$5 \cdot 10^{-4}$
SVHN	3.640 ± 0.090	3.589 ± 0.122	0.01

Table 2. Mean errors for standard BP ($\beta = 0$) and invariant BP ($\beta > 0$) and the best β on different datasets, **with dropout**.

* means statistically significant according to the Wilcoxon rank-sum test ($\alpha = 0.05$).

	Standard BP	Invariant BP	best β
MNIST	0.410 ± 0.039	0.371 ± 0.036 *	$2 \cdot 10^{-4}$
CIFAR-10	15.90 ± 0.223	15.67 ± 0.198 *	$5 \cdot 10^{-5}$
CIFAR-100	46.06 ± 0.330	45.13 ± 0.270 *	$5 \cdot 10^{-5}$
SVHN	3.570 ± 0.052	3.517 ± 0.065	$1 \cdot 10^{-3}$

length 256. In this case we trained the classifier for 800 epochs with $\gamma = 0.99$, so $0.99^{800} \approx 0.0003$ as well as for the MNIST database.

SVHN

Street View House Numbers (SVHN) is another dataset widely used in image classification. It contains more than 600 thousand coloured images of digits from house numbers. As well as CIFAR dataset, these images also have the size $32 \times 32 \times 3$. To obtain the validation set and normalizing the images we followed the procedure described in (Goodfellow et al., 2013). Instead of subtracting the per-pixel mean, the authors perform local contrast normalization. We employed the same network structure as for CIFAR, but given that we have 10 times more samples, we added one more FC layer of the same size 256. For the same reason we trained the classifier for only 80 epochs, decreasing the learning rates on 10% after each of them.

5.2. Standard BP and Invariant BP

The final results of classification accuracy on full datasets are summarized in Tables 1 and 2. We can observe a decrease of the error with respect to both versions of BP with and without dropout for all datasets, except SVHN. The best result is achieved for the combination of both IBP and dropout regularizers. Notice that in all cases the best value of β in a combination with dropout is 10 times lower than the best value without it. Thus, when dropout is used, less additional regularization is required. At the same time, the absolute improvement of IBP remains approximately the same regardless of what dropout rate is used.

As we see from the tables, additional fully connected layer on SVHN dataset lead to much larger optimal values of

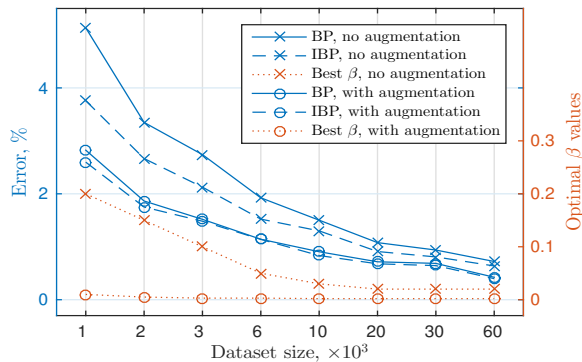


Figure 2. Classification errors on the MNIST subsets of different size for standard BP and invariant BP with and without data augmentation. The corresponding optimal values of β is shown by the dotted lines. Smaller dataset sizes require larger β and get more accuracy improvement.

β compared with *CIFAR*. However, even with additional layer the network did not overfit: the obtained improvement was not statistically significant. Thus, we see that the larger the dataset is, the less it overfits, and the less improvement we can obtain from regularization. In this case if the dataset is complex enough, we can employ larger networks that can capture these complex relations between input data and output classes. While IBP does not give any improvement of accuracy in this case, it still makes the classifier more robust to noise.

5.3. Dataset size and data augmentation

We have also established how the dataset size and data augmentation affects the IBP improvement. We performed these experiments on MNIST dataset using the same structure as described in the section 5.1. The results are summarised on the Fig. 2. It shows the test errors for the training subsets of different size and the corresponding best values of β . We see that smaller datasets require more regularization (i.e., larger β), and the corresponding absolute accuracy improvement is higher. The relative improvement is also higher: in the case of not augmented datasets it is 27% for 1000 samples and only 12% for 60000. This result matches with the observation we have made for the SVHN dataset.

Data augmentation improves the accuracy even more than IBP. Since these two methods aim to solve the same problem, they compensate each other, and the improvement of IBP in a combination with data augmentation is much less. As it is seen from the Fig. 2, the optimal value of β is also at least 10 times lower. Thus, IBP is the most efficient when in the case of small datasets when it is not possible to generate additional samples.

Table 3. Computation time of one epoch, seconds

	BP	IBP	IBP/BP ratio
MNIST	3.80	5.76	1.52
CIFAR-10	5.01	7.46	1.53
CIFAR-100	5.01	7.64	1.53
SVHN	58.6	90.9	1.55

5.4. Loss functions behavior

It is also interesting to look at the plots of the main and additional loss functions. Plots (3(a)) and (3(b)) demonstrate their curves obtained during the CIFAR-10 training process. We can see that standard backpropagation (blue curves) achieves the lowest value of main loss L and the highest value the test error. It is a clear sign of overfitting. From (3(a)) we can also see that IBP (as well as dropout) acts as a regularizer, increasing L and decreasing the test error. Fig. 3(b) confirms that IBP decreases the additional loss \tilde{L} , and the larger is β , the lower is \tilde{L} .

5.5. Robustness to noise

Two other plots (4(a)) and (4(b)) show how the accuracy degrades when we add Gaussian noise to the test set. For the experiment we used the classifiers for CIFAR-10 and CIFAR-100 datasets, obtained in the section 5.2. We can clearly see that the green curves that correspond to the classifiers with the largest β have the smallest slope. Pure dropout gives higher accuracy than standard BP, but as we add noise, this classifier degrades faster. At the same time, in the case of CIFAR-100 IBP allows us to preserve its advantage over standard BP when noise is added. These results demonstrate that the theoretically desired properties are observed in practice.

5.6. Computation time

As we see from Table 3, the additional time is about 53%. It is slightly less than approximated 66%, because both versions contain fixed time procedures such as batch composing, data augmentation, etc. Thus, we experimentally confirmed that the additionally required time is not more than theoretical 66%.

5.7. Tangent BP and Invariant BP

We implemented the tangent propagation algorithm and performed some experiments on MNIST and CIFAR-10 datasets. In these experiments we used 5 tangent vectors, corresponding to x and y shifts, x and y scaling and rotation. Since the tangent vectors have to be precomputed in advance, we could not use data augmentation implemented as transformation on a fly, so we did not use data augmentation at all. In order to simplify the design, we did not use

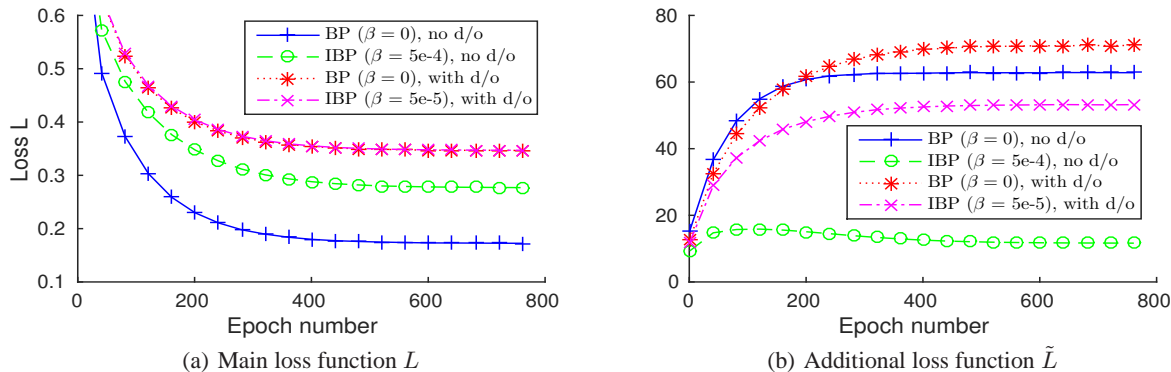


Figure 3. The plots of the loss function values on CIFAR-10 dataset for standard BP and invariant BP with and without dropout. IBP increases main loss L , but decreases additional loss \tilde{L} . The large is β , the lower is \tilde{L} .

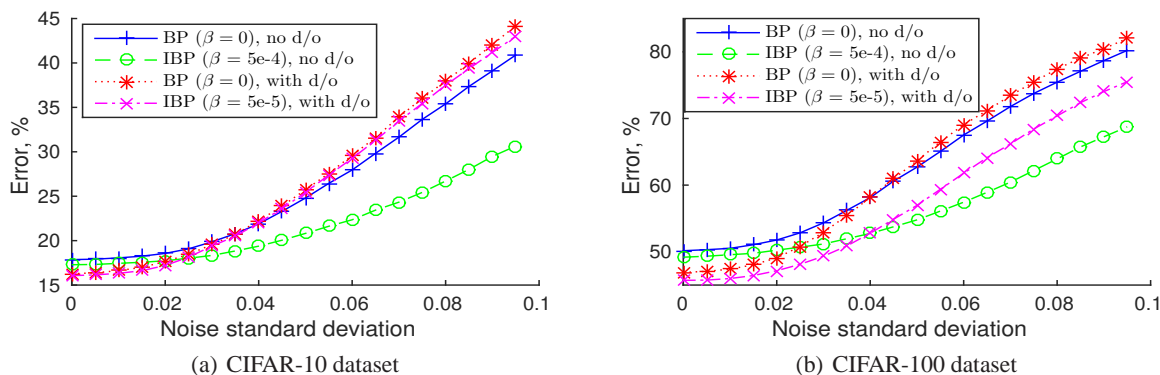


Figure 4. The plots of classification errors as functions of noise of the test set for standard BP and invariant BP with and without dropout. In all cases the IBP error increases slower than the corresponding BP error, what demonstrates the robustness of the IBP classifier.

the dropout as well. First, we estimated the performance of tangent BP on simple neural networks with only fully connected layers. We used 2 internal layers of size 256 for MNIST and 3 layers of the same size for CIFAR. The results are summarized in Table 4. We see that the accuracy is far from the best results, but the relative improvement of the tangent BP is about 2 times less than IBP. Tangent BP also required 3.8 more time for 1 epoch than standard BP.

Next, we performed the experiments on the same network structures that were used to obtain the results from Tables 1 and 2. We did not use data augmentation and dropout, all parameters were the same. Unfortunately, we could not find any value of $\beta > 0$ that would give a statistically significant improvement of classification accuracy. Thus, we have demonstrated that on these 2 datasets IBP outperforms tangent BP in terms of accuracy, time and convenience.

6. Conclusion

We have described an invariant backpropagation algorithm (IBP): extension of the standard backpropagation algorithm

Table 4. Mean errors for standard BP, tangent BP and invariant BP on the neural networks with only fully connected layers

	Standard BP	Tangent BP	IBP
MNIST	2.16 ± 0.11	1.96 ± 0.06	1.67 ± 0.07
CIFAR-10	49.85 ± 0.35	46.29 ± 0.26	44.06 ± 0.38

for learning a neural network that is robust to variations in the initial data. Our algorithm requires an additional forward pass for the input vector derivatives and one more calculation of derivatives. Therefore, it is easy for implementation and only requires around 50% more computation time. It can also be applied together with any other methods of regularization. The experiments have demonstrated an improvement of classification accuracy and robustness to noise. The algorithm might be especially useful in the cases of small datasets when additional data generation is not possible. We believe that its properties will make it useful to improve practical usage of neural networks in the areas of image classification, voice recognition and others.

References

- Ahonen, Timo, Matas, Jiří, He, Chu, and Pietikäinen, Matti. Rotation invariant image description with local binary pattern histogram fourier features. In *Image Analysis 2009*, pp. 61–70. 2009.
- Bay, Herbert, Tuytelaars, Tinne, and Van Gool, Luc. Surf: Speeded up robust features. In *ECCV 2006*, pp. 404–417. 2006.
- Deng, Li, Li, Jinyu, Huang, Jui-Ting, Yao, Kaisheng, Yu, Dong, Seide, Frank, Seltzer, Michael, Zweig, Geoff, He, Xiaodong, Williams, Jason, et al. Recent advances in deep learning for speech research at microsoft. In *Acoustics, Speech and Signal Processing (ICASSP), 2013 IEEE International Conference on*, pp. 8604–8608. IEEE, 2013.
- Fergus, Robert, Perona, Pietro, and Zisserman, Andrew. Object class recognition by unsupervised scale-invariant learning. In *CVPR 2003*, 2003.
- Goodfellow, Ian J, Warde-Farley, David, Mirza, Mehdi, Courville, Aaron, and Bengio, Yoshua. Maxout networks. *arXiv preprint arXiv:1302.4389*, 2013.
- Hinton, Geoffrey E, Srivastava, Nitish, Krizhevsky, Alex, Sutskever, Ilya, and Salakhutdinov, Ruslan R. Improving neural networks by preventing co-adaptation of feature detectors. *arXiv preprint arXiv:1207.0580*, 2012.
- Karpathy, Andrej and Fei-Fei, Li. Deep visual-semantic alignments for generating image descriptions. *arXiv preprint arXiv:1412.2306*, 2014.
- Krizhevsky, Alex. Learning multiple layers of features from tiny images. *Master's thesis, University of Toronto*, 2009.
- LeCun, Yann, Bottou, Léon, Bengio, Yoshua, and Haffner, Patrick. Gradient-based learning applied to document recognition. *Proceedings of the IEEE*, 86(11):2278–2324, 1998.
- Lee, Chen-Yu, Xie, Saining, Gallagher, Patrick, Zhang, Zhengyou, and Tu, Zhuowen. Deeply-supervised nets. *arXiv preprint arXiv:1409.5185*, 2014.
- Lin, Min, Chen, Qiang, and Yan, Shuicheng. Network in network. *arXiv preprint arXiv:1312.4400*, 2014.
- Lowe, David G. Distinctive image features from scale-invariant keypoints. *International Journal of Computer Vision*, 60(2):91–110, 2004.
- Nair, Vinod and Hinton, Geoffrey E. Rectified linear units improve restricted boltzmann machines. In *ICML 2010*, pp. 807–814, 2010.
- Norouzi, Mohammad, Ranjbar, Mani, and Mori, Greg. Stacks of convolutional restricted boltzmann machines for shift-invariant feature learning. In *CVPR 2009*, pp. 2735–2742, 2009.
- Ranzato, Marc’ Aurelio, Huang, Fu Jie, Boureau, Y-Lan, and Lecun, Yann. Unsupervised learning of invariant feature hierarchies with applications to object recognition. In *CVPR 2007*, pp. 1–8, 2007.
- Rifai, Salah, Vincent, Pascal, Muller, Xavier, Glorot, Xavier, and Bengio, Yoshua. Contractive auto-encoders: Explicit invariance during feature extraction. In *ICML 2011*, pp. 833–840, 2011.
- Simard, Patrice Y, LeCun, Yann A, Denker, John S, and Victorri, Bernard. Transformation invariance in pattern recognition—tangent distance and tangent propagation. In *Neural networks: tricks of the trade*, pp. 235–269. Springer, 2012.
- Szegedy, Christian, Liu, Wei, Jia, Yangqing, Sermanet, Pierre, Reed, Scott, Anguelov, Dragomir, Erhan, Dumitru, Vanhoucke, Vincent, and Rabinovich, Andrew. Going deeper with convolutions. *arXiv preprint arXiv:1409.4842*, 2014.
- Wan, Li, Zeiler, Matthew, Zhang, Sixin, Cun, Yann L, and Fergus, Rob. Regularization of Neural Networks using DropConnect. In *ICML 2013*, pp. 1058–1066, 2013.
- Zeiler, Matthew D and Fergus, Rob. Stochastic pooling for regularization of deep convolutional neural networks. *arXiv preprint arXiv:1301.3557*, 2013.